

# Inhibition of Microsomal Epoxide Hydrolases by Ureas, Amides, and Amines

Christophe Morisseau, John W. Newman, Deanna L. Dowdy,  
Marvin H. Goodrow, and Bruce D. Hammock\*

Department of Entomology and University of California Cancer Center, University of California,  
Davis, California 95616

Received August 11, 2000

The microsomal epoxide hydrolase (mEH) plays a significant role in the metabolism of xenobiotics such as polyaromatic toxicants. Additionally, polymorphism studies have underlined a potential role of this enzyme in relation to several diseases, such as emphysema, spontaneous abortion, and several forms of cancer. To provide new tools for studying the function of mEH, inhibition of this enzyme was investigated. Inhibition of recombinant rat and human mEH was achieved using primary ureas, amides, and amines. Several of these compounds are more potent than previously published inhibitors. Elaidamide, the most potent inhibitor that is obtained, has a  $K_i$  of 70 nM for recombinant rat mEH. This compound interacts with the enzyme forming a noncovalent complex, and blocks substrate turnover through an apparent mix of competitive and noncompetitive inhibition kinetics. Furthermore, in insect cell cultures expressing rat mEH, elaidamide enhances the toxicity effects of epoxide-containing xenobiotics. These inhibitors could be valuable tools for investigating the physiological and toxicological roles of mEH.

## Introduction

Epoxides are highly strained three-membered cyclic ethers that are often electrophilically reactive mutagens, carcinogens, or cytotoxins (1). Epoxide hydrolases (EH, EC 3.3.2.3) catalyze the hydrolysis of epoxides or arene oxides to their corresponding diols (2). Microsomal epoxide hydrolase (mEH) is a key hepatic enzyme involved in the metabolism of numerous xenobiotics, such as polyaromatic hydrocarbons, which undergo cytochrome-dependent epoxidation (3, 4). Additionally, mEH is likely involved in the extrahepatic metabolism of these agents, such as naphthalene in the lungs (5). Generally, the conversion of epoxides to diols results in less mutagenic or carcinogenic compounds. However, in some cases, as for benzo[a]pyrene 4,5-oxide, diol formation can lead to the stabilization of a secondary epoxide, increasing the mutagenic and carcinogenic potential of the product (6). The role of mEH in xenobiotic detoxication is also supported by recent polymorphism studies showing a relationship between this enzyme and susceptibility to emphysema (7) and several forms of cancer (8). Despite the fact that mEH knockout mice do not present an obvious phenotype (9), there are several points suggesting an endogenous role for this enzyme. A potential role of mEH in sexual development is supported by the facts that androstene oxide is a very good mEH substrate (10), and that mEH is an apparent subunit of the anti-estrogen-binding site (11). Such a role could be related to the observed relation between mEH polymorphism and spontaneous abortion (12), which has been reported to occur in more than 10% of recognized pregnancies (13).

Over the past decade, mEH was also described as mediating the transport of bile acid into hepatocytes (14, 15). The mechanism by which mEH participates in bile absorption is not known. Obtaining potent mEH inhibitors will provide new tools for better understanding the multiple roles of this enzyme.

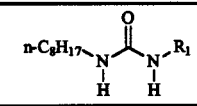
Over the years, several mEH inhibitors have been described, including 1,1,1-trichloro-2,3-epoxypropane (16), cyclohexene oxide (17), several other cycloalkene oxides (18), and valpromide (19), and more recently, our laboratory described mEH inhibition by metals (20). The former compounds, which are inefficient *in vivo*, are in fact substrates of mEH and give only transient inhibition of this enzyme *in vitro* (2). Valpromide affects the normal metabolism of carbamazepine by inhibiting the mEH *in vivo* (19). However, the anticonvulsant properties of valpromide could induce undesirable secondary effects if it is used as a mEH inhibitor. We recently developed new inhibitors for the soluble epoxide hydrolase (sEH), an enzyme distantly related to mEH (21). These inhibitors are based on urea, carbamate, or amide central functions. These inhibitors act by mimicking a transition state in the enzyme catalytic mechanism of epoxide hydrolysis (22). Because sEH and mEH have similar mechanisms of catalysis (3, 23), one could expect that urea and urea-like compounds would be inhibitors of the mEH also. We describe herein the discovery of new potent and stable inhibitors of mEH and their application in one *in vitro* model.

## Materials and Methods

**Chemicals.** General laboratory reagents were purchased from either Aldrich (Milwaukee, WI) or Sigma (St. Louis, MO), and used without further purification. Compounds 15–29, 40,

\* To whom correspondence should be addressed: Department of Entomology, University of California, Davis, CA 95616. Phone: (530) 752-7519. Fax: (530) 752-1537. E-mail: bdhammock@ucdavis.edu.

**Table 1. Inhibition of Rat mEH c-SO Hydrolysis by *N*-Octylureas**

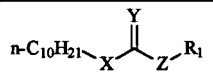
		No.	m. p. <sup>a</sup> (°C)	Yield (%)	IC <sub>50</sub> <sup>b</sup> (μM)
R <sub>1</sub> :	H	1	96.0-97.5	90	73 ± 1
	CH <sub>3</sub>	2	71.0-72.0	96	240 ± 5
	CH <sub>2</sub> CH <sub>3</sub>	3	58.0-59.0	87	> 500
	CH <sub>2</sub> CH <sub>2</sub> CH <sub>3</sub>	4	67.0-68.0	92	> 500
	CH <sub>2</sub> -CH=CH <sub>2</sub>	5	65.5-66.5	89	> 500
	CH-(CH <sub>3</sub> ) <sub>2</sub>	6	70.0-71.0	94	> 500
		7	57.5-59.0	95	171 ± 2
		8	90.0-91.0	90	> 500
		9	79.0-80.0	91	> 500

<sup>a</sup> Melting points (mp) are uncorrected. <sup>b</sup> The enzyme and the inhibitor are incubated together for 5 min at 30 °C before the addition of substrate (c-SO, 50 μM). Results are means ± SD of three separate experiments.

and **41** were obtained from Aldrich, while compound **37** was purchased from Sigma. Compounds **1–10**, **13**, and **39** were synthesized by the condensation of the appropriate isocyanate and amine, whereas compounds **11** and **12** were synthesized by the condensation of the appropriate isocyanate and alcohol as previously described (21). Compounds **14**, **30–36**, and **38** were synthesized by the condensation of the appropriate acyl chloride and ammonia as described by Roe et al. (24). Reaction products were purified by recrystallization. Purities of >95% were obtained for all of the compounds that were studied. Assignment of purities was carried out using NMR and mass spectroscopy data. In addition to sharp melting points and single spots on silica gel TLC, the obtained products were characterized using <sup>1</sup>H and/or <sup>13</sup>C NMR (General Electric QE-300 instrument), infrared, and mass spectroscopy [for GC/MS, Hewlett-Packard 6890 gas chromatograph (San Jose, CA) equipped with a 30 m × 0.25 mm × 0.25 μm film DB-5ms column (J&W Scientific, Folsom, CA) and a 5973 mass spectra detector; for electrospray ionization (ESI-MS), positive mode Fisons Quattro BQ apparatus (Altrancham, England), 5 μL/min flow of a 1:1:0.05 (v:v:v) acetonitrile/water/formic acid mixture, with a cone voltage of 50 V; fast atom bombardment mass spectra were generated on a Kratos MS-50 mass spectrometer (Kratos Analytical, Manchester, U.K.)]. Melting point and reaction yields are listed in Tables 1–3. Acquired IR, NMR, and MS data used for structural confirmation can be found as Supporting Information. The detailed syntheses of two ureas and an amide representing these reaction pathways are included below.

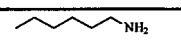
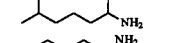
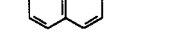
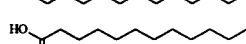
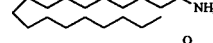
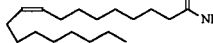
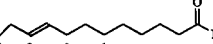
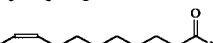
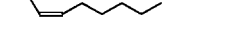
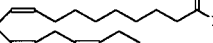
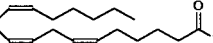
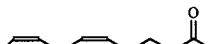
**Compound 1 (N-Octylurea).** Octyl isocyanate (0.88 mL, 0.77 g, 5.0 mmol) and 6 mL of 1 M ammonium hydroxide were vigorously shaken for 3 h. The precipitate was collected, washed with water followed by an acetone wash, and vacuum-oven dried to obtain 0.77 g (90%) of **1**. The isolated solid had an mp of 96.0–97.5 °C, which was unchanged by recrystallizations from either a methanol/water mixture (5:2, v:v) or a hexanes/ethyl acetate mixture (4:1, v:v): IR (KBr) 3393 (s, NH), 1657 (s, C=O), 1603 (vs), 1537 cm<sup>-1</sup> (s, amide II); <sup>1</sup>H NMR (CDCl<sub>3</sub>) δ 4.5 (m, 1 H, NH), 4.3 (m, 2 H, NH<sub>2</sub>), 3.15 (dd, *J* = 7.0, 6.0 Hz, 2 H, CH<sub>2</sub>-1), 1.5 (m, 2 H, CH<sub>2</sub>-2), 1.3 (m, 10 H, CH<sub>2</sub>-3–7), 0.88 (t, *J* = 6.6 Hz, 3 H, CH<sub>3</sub>); <sup>13</sup>C NMR (DMSO-*d*<sub>6</sub>) δ 158.7 (C=O), 39.3 (C-1), 31.2 (C-2), 30.0 (C-4), 28.8 (C-5 or -6), 28.7 (C-5 or -6), 26.4 (C-3), 22.1 (C-7), 13.8 (C-8); fast atom bombardment MS *m/z* (relative intensity) 345 (2M + H<sup>+</sup>, 10%), 173 (M + H<sup>+</sup>, 100%).

**Table 2. Inhibition of RmEH by Several Pharmacophores**

					m. p. <sup>a</sup> (°C)	Yield (%)	IC <sub>50</sub> <sup>b</sup> (μM)
X	Y	Z	R <sub>1</sub>	No.			
NH	O	NH	CH <sub>3</sub>	10	77.5-79.0	84	190 ± 8
O	O	NH	CH <sub>3</sub>	11	43.5-44.5	60	34 ± 2
NH	O	O	CH <sub>3</sub>	12	65.0-67.0	54	> 500
NH	O	NH	H	13	93.0-94.0	67	12 ± 2
CH <sub>2</sub>	O	NH	H	14	98.0-99.0	92	2.34 ± 0.05
CH <sub>2</sub>	O	O	H	15	–	–	> 500
CH <sub>2</sub>	O	O	CH <sub>3</sub>	16	–	–	> 500
CH <sub>2</sub>	2H	NH	H	17	–	–	2.54 ± 0.04
CH <sub>2</sub>	2H	NH	CH <sub>3</sub>	18	–	–	4.06 ± 0.05
CH <sub>2</sub>	2H	N	(CH <sub>3</sub> ) <sub>2</sub>	19	–	–	103.9 ± 0.2
CH <sub>2</sub>	2H	O	H	20	–	–	> 500
CH <sub>2</sub>	2H	S	H	21	–	–	> 500
CH <sub>2</sub>	2H	Br		22	–	–	> 500
CH <sub>2</sub>	CN			23	–	–	> 500
CH <sub>2</sub>	2H	CH <sub>2</sub>	H	24	–	–	> 500

<sup>a</sup> Melting points (mp) are uncorrected. “–” indicated that the melting points of the commercial compound were not measured. <sup>b</sup> The enzyme and the inhibitor are incubated together for 5 min at 30 °C before the addition of substrate (c-SO, 50 μM). Results are means ± SD of three separate experiments.

**Table 3. Inhibition of Rat mEH by Amines and Amides with Diverse Alkyl Chains**

Structure	No.	m. p. (°C)	Yield (%)	IC <sub>50</sub> (μM)
	25	–	–	160 ± 3
	26	–	–	38.7 ± 0.7
	27	–	–	> 500
	28	–	–	69 ± 6
	29	–	–	> 100
	30	104-105	88	20.4 ± 0.5
	31	–	–	1.28 ± 0.04
	32	89.0-90.0	90	1.3 ± 0.1
	33	oil	92	0.82 ± 0.01
	34	77.0-78.0	95	1.1 ± 0.1
	35	oil	91	1.2 ± 0.1
	36	oil	93	1.33 ± 0.05
	37	–	–	0.98 ± 0.04
	38	oil	88	2.1 ± 0.1

**Compound 7 (N-Cyclopropyl-N'-octylurea).** To 0.115 g (2.00 mmol) of cyclopropylamine in 10 mL of hexane were added 0.310 g (2.00 mmol) of octyl isocyanate and 1 drop of 1,8-

diazabicyclo[5.4.0]undec-7-ene. After 1 day at ambient temperature, compound **7** was obtained (0.405 g, 95%) as white crystals: mp 57.5–59.0 °C; IR (KBr) 3339 (m, NH), 1626 (vs, C=O), 1573 cm<sup>-1</sup> (s, amide II); <sup>1</sup>H NMR (CDCl<sub>3</sub>) δ 5.17 (br, 2 H, 2 NH), 3.20 (dt, *J* = 6.6, 6.3 Hz, 2 H, CH<sub>2</sub>-1), 2.4 (m, 1 H, CH), 1.5 (m, 2 H, CH<sub>2</sub>-2), 1.3 (m, 10 H, CH<sub>2</sub>-3–7), 0.88 (t, 3 H, *J* = 6.5 Hz, CH<sub>3</sub>), 0.7 (m, 2 H, cyclopropyl), 0.5 (m, 2 H, cyclopropyl); <sup>13</sup>C NMR (CDCl<sub>3</sub>) δ 159.3 (C=O), 40.2 (C-1), 31.7 (C-6), 30.3 (C-2), 29.2 (C-4), 29.1 (C-5), 26.8 (C-3), 22.5 (C-7), 22.3 (C-1'), 13.9 (C-8), 7.1 (C-2',3'); fast atom bombardment MS *m/z* (relative intensity) 425 (2M + H<sup>+</sup>, 16%), 213 (M + H<sup>+</sup>, 86%), 58 (cyclopropyl-NH<sub>2</sub> + H<sup>+</sup>, 100%).

**Compound 32 (Elaidamide).** To a stirred cold solution of 0.60 g (2 mmol) of elaidoyl chloride (Nu-Chek Prep, Elysian, MN) in 5 mL of chloroform was added ammonia (4.4 mmol) in 2.2 mL of a 2.0 M solution in ethanol. After being stirred at room temperature for 1 h, the solution was washed with water, acidic water, water, and brine. The organic layer was dried and evaporated. The resulting solid was recrystallized twice from hot hexane. The resulting white crystal (0.51 g, 90% yield) had an mp of 89–90 °C and gave a single spot on TLC (*R*<sub>f</sub> = 0.32 with ethyl acetate as the solvent and phosphomolybdic acid as the stain): GC/MS *m/z* (relative intensity) 281 ([M]<sup>+</sup> (C<sub>18</sub>H<sub>35</sub>NO), 12%), 264 ([M - NH<sub>3</sub>]<sup>+</sup>, 8%), 168 ([M - C<sub>8</sub>H<sub>17</sub>]<sup>+</sup>, 5%), 128 ([M - C<sub>11</sub>H<sub>21</sub>]<sup>+</sup>, 10%), 59 ([M - C<sub>16</sub>H<sub>30</sub>]<sup>+</sup>, 10%); ESI-MS *m/z* 563.7 ([2M + H]<sup>+</sup>), 282.5 ([M + H]<sup>+</sup>); <sup>1</sup>H NMR (CDCl<sub>3</sub>) δ 5.58 (bs, 1 H, NH), 5.43 (bs, 1 H, NH), 5.37 (t, *J* = 4.0 Hz, 2 H, CH=CH), 2.23 [t, *J* = 7.6 Hz, 3 H, CH<sub>2</sub>(C=O)NR<sub>2</sub>], 1.95 (m, 4 H, CH<sub>2</sub>C=CC<sub>2</sub>H<sub>5</sub>), 1.61 [m, 2 H, CH<sub>2</sub>C(C=O)NR<sub>2</sub>], 1.16–1.33 (m, 20 H, CH<sub>2</sub>), 0.87 (t, *J* = 6.8 Hz, 3 H, CH<sub>3</sub>).

**Enzyme Preparation.** Recombinant rat mEH (RmEH) and human mEH (HmEH) were produced in a baculovirus expression system as described previously (25–27). High Five insect cell cultures (derived from *Trichoplusia ni*; Invitrogen, San Diego, CA) were infected with the appropriate recombinant baculovirus at a multiplicity of infection of 0.1 virus per cell. The mEH enzyme activity was retained in the cells. After incubation for 90–96 h at 28 °C, cells were harvested by centrifugation (100*g* for 10 min at 4 °C). After resuspension in chilled 0.1 M Tris/HCl buffer (pH 9.0) containing 1 mM phenylmethanesulfonyl fluoride, EDTA, dithiothreitol, and 1% Lubrol PX (v:v), cells were disrupted using a Polytron homogenizer (9000 rpm for 30 s). The homogenate was centrifuged at 12000*g* for 20 min at 4 °C. The supernatant (crude extract) containing the mEH activity was frozen at –80 °C until it was used. Under these conditions, no loss of activity was observed even after 1 year in the freezer. However, substantial loss of activity was observed after several freeze/thaw cycles (~25% activity lost after five cycles). Protein concentrations were determined using the Bio-Rad Coomassie assay using Fraction V bovine serum albumin (BSA) as the calibrating standard.

**IC<sub>50</sub> Assay Conditions.** IC<sub>50</sub> values were determined using [<sup>3</sup>H]-*cis*-stilbene oxide (c-SO) as the substrate (1). The enzymes (1 nmol min<sup>-1</sup> mL<sup>-1</sup>) were incubated with inhibitors for 5 min in 0.1 M Tris/HCl buffer (pH 9.0) containing 0.1 mg/mL BSA at 30 °C before substrate introduction ([S]<sub>final</sub> = 50 μM). After 5 min, the reaction was quenched by addition of 250 μL of isooctane, which extracts the remaining epoxide from the aqueous phase. The activity was followed by measuring the quantity of radioactive diol formed in the aqueous phase using a liquid scintillation counter (Wallac model 1409, Gaithersburg, MD). Assays were performed in triplicate. The median inhibitor concentrations (IC<sub>50</sub>) were determined by regression of at least five points in the linear region of the curve on either side of the IC<sub>50</sub>. The curve was generated from at least three separate runs, each in triplicate, to obtain the SD given in the tables.

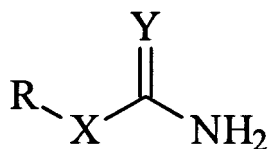
**Kinetic Assay Conditions.** Dissociation constants were determined following the method described for linear mixed-type inhibition (28) using *cis*-stilbene oxide as the substrate. Inhibitors at concentrations between 0 and 10 μM were incubated in triplicate for 5 min in 0.1 M Tris/HCl buffer (pH 9.0) at 30 °C with the RmEH diluted to give a maximal rate of 0.4

nmol min<sup>-1</sup> mL<sup>-1</sup> for the substrate c-SO. Substrate (1.5 < [S]<sub>final</sub> < 50 μM) was then added. Velocity was measured as described under IC<sub>50</sub> Assay Conditions. For each inhibitor concentration, linear relations are produced between the inverse of the velocity and the inverse substrate concentration (Lineweaver–Burk representation). The plots of the slopes and intercepts of these lines as functions of the inhibitor concentration allow the determination of *K*<sub>i</sub> and the factor α, respectively (28). The affinity modulation factor α describes the amplitude of change in the dissociation constant *K*<sub>s</sub> when the inhibitor occupies the enzyme (28). The results are presented as means ± SD of three separate determinations of *K*<sub>i</sub> and α.

**Cytotoxicity Assay.** Toxicity studies were performed in cultured cells of *Spodoptera frugiperda* (Sf-21) as previously described (26). Briefly, the cells were infected with baculovirus expressing RmEH or β-galactosidase (Lac Z) as a control, at a multiplicity of infection of 0.1. For assays with naphthalene, the cells were coinfecting with a virus expressing a rat P450 1A1/reductase chimeric enzyme, and the medium was supplemented with 1.0 μg/mL hemin (26). Under these conditions, 48 h postinfection, a P450 1A1/reductase activity of 120 ± 20 pmol min<sup>-1</sup> mg<sup>-1</sup> was found using ethoxyresorufin as the substrate (38). Similarly, mEH activity of 2000 ± 200 pmol min<sup>-1</sup> mg<sup>-1</sup> was found using c-SO as the substrate (1). Compounds (*cis*-stilbene oxide or naphthalene) were administered to cells (0–1 mM final concentration) 48 h postinfection, in the absence or presence of 100 μM elaidamide **34**. After incubation for 24 h at 27 °C, the remaining viable cells were quantified by incubation with 3-(4,5-dimethylthiazol-2-yl)-2,5-diphenylterazolium bromide (MTT, 1 mg/mL final concentration) for 2 h. The cells were lysed with a 10% sodium dodecyl sulfate solution in a 1:1 dimethylformamide/water mixture (pH 4.5) over the course of 12 h in the dark. The formazan product was quantified by measuring the absorbance at 560 nm. Viability was normalized to cells treated with vehicle (1% dimethyl sulfoxide) only. Toxicity data are representative of three independent experiments.

## Results and Discussion

**Structure Optimization.** In a preliminary study, compounds identified as sEH inhibitors (21) failed to inhibit RmEH at 500 μM (data not shown). However, the negative sEH inhibition set contained a number of alkyl ureas and carbamates, some of which were found to be good RmEH inhibitors. To explore the effect of N-substitution, 10 unbranched *N*-octylureas with different *N'*-groups (**1–9**) were tested (Table 1). Inhibition was only observed for small *N'*-substituents, and the best inhibition was obtained with the primary urea **1**, indicating the necessity of a single substitution on the urea pharmacophore. This result was consistent with the observation that some unsubstituted amides can inhibit mEH (19, 29, 30). To further optimize the pharmacophore for inhibition, a series of structural analogues were tested (Table 2). Compared with that of urea **10**, the replacement of the nitrogen adjacent to the large alkyl chain with an oxygen to give carbamate **11** increased inhibitor potency, while the reverse carbamate **12** showed no inhibition, suggesting the necessity of a polar terminal group. Compared to that of urea **13**, the replacement of the nitrogen on the large side with a methylene to give amide **14** resulted in a 5-fold increase in inhibitor potency. The further replacement of the “small” side nitrogen with oxygen to give acid **15** or ester **16** resulted in a loss in the level of inhibition compared to that of **13** or **10**, respectively. Compared to that of amide **14**, the elimination of the carbonyl group gives an amine **17** with a similar potency, indicating that the carbonyl is not necessary for inhibition. As observed for ureas (Table 1),



R: alkyl group.

X:  $\text{CH}_2 > \text{O} > \text{NH}$

Y:  $\text{O} \cong \text{H}_2$ .

**Figure 1.** Theoretical optimal structure of mEH inhibitors described herein.

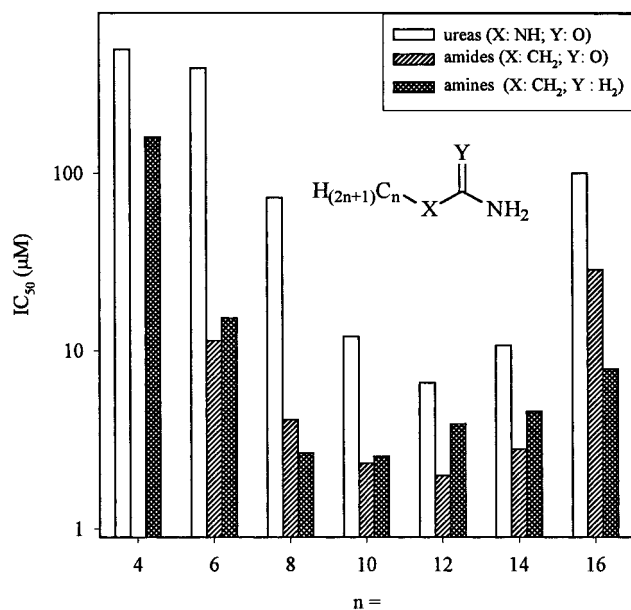


**Figure 2.** Effect of alkyl chain length on the potency of ureas, amides, and amines as inhibitors of mEH.

better inhibition is obtained for a monosubstituted amine **17** than for the di- and trisubstituted ones (**18** and **19**). Compared to amine **17**, the replacement of the terminal group with alcohol (**20**), thiol (**21**), bromide (**22**), nitrile (**23**), or hydrogen (**24**) resulted in a loss of inhibition. These results are summarized in Figure 1. The optimal pharmacophore structure should have a terminal  $\text{NH}_2$  function on a long alkyl chain; the presence of a carbonyl group  $\alpha$  to the terminal  $\text{NH}_2$  is not necessary. The presence of either  $\text{CH}_2$ ,  $\text{NH}$ , or  $\text{O}$  at position  $X$  could not be distinguished in terms of inhibition in this series. Interestingly, the good inhibitors of the mEH described by Figure 1 are bad inhibitors of sEH, which required the presence of 1,3-disubstitution around the central urea pharmacophore (*21*), while good sEH inhibitors are bad mEH inhibitors. These results indicate that, as for substrate selectivity and specificity (*1*), sEH and mEH seem to have a different yet complementary spectrum regarding structure–activity relationship among inhibitors.

To further optimize the inhibitor structure, we then investigated the alkyl chain length. Primary ureas, amides, and amines with a linear saturated chain from 4 to 16 carbons long were tested as inhibitors of mEH. The results are displayed in Figure 2. Overall, the relationship of chain length to inhibitory potency was similar for the three compound classes with an optimum 10–12 ( $n$ ). Moreover, better inhibition potencies are

obtained for the amides and amines than for the ureas, again deviating from the findings with sEH (*21*), indicating that for the atom at position  $X$  (Figure 1) a carbon gives better mEH inhibition than a nitrogen. Additional side chain optimization was attempted with several structural changes (Table 3). Compared to that of compound **25**, the presence of methyl branches on **26** increased the inhibitor potency by 4-fold. The replacement of the alkyl chain with aromatic rings (**27**) resulted in a loss of inhibition. Such results were unexpected in light of the fact that polyaromatic oxides are good mEH substrates (*3, 4*). Compared to the aliphatic amine **17**, the presence of a terminal amino (**28**) or carboxylic (**29**) group dramatically reduced the inhibition potency, indicating a requirement for a hydrophobic side chain. Compared to that of compound **30**, the presence of one double bond either *cis* (**31**) or *trans* (**32**) produced a 15-fold increase in inhibition potency. However, the presence of additional double bonds (**33–38**) resulted in little improvement in the inhibitor potency. These data show that the side chain of the optimal mEH inhibitor (Figure 1) should be aliphatic and hydrophobic, and suggest that this aliphatic chain should be 8–12 carbons long or longer if it has olefin interruption at or near the 10th carbon.

Several fatty acid amides, such as **31**, **33**, and **37**, are endogenous signaling lipids which generate several pharmacological effects in mammals, including sleep (*31*) and analgesia (*32*). We initially developed the hypothesis that inhibition of mEH or a related protein could be involved in the sleep-inducing phenomena because oleamide **31**, in addition to inhibiting mEH, is described as a brain lipid that induces sleep (*31*) and because mEH is present in the brain (*33*). We tested this hypothesis by assessing the inhibition potency of related compounds, such as **32**, reported to not induce sleep (*34, 35*). Several of these compounds were good inhibitors of the mEH, thus failing to support our hypothesis.

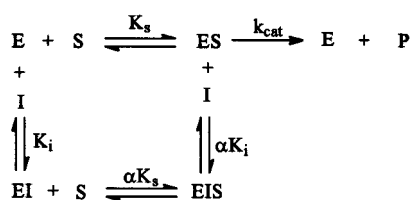
**Kinetics of Inhibition.** Compared to 1,1,1-trichloro-2,3-epoxypropane **40**, cyclohexene oxide **41**, and valpromide **42**, the most potent mEH inhibitors reported previously (*16–19*), the best new urea **39**, amide **32**, and amine **17** have similar or lower  $\text{IC}_{50}$  values after incubation for 5 min (Table 4). After 30 min, 2- and 5-fold increases in the  $\text{IC}_{50}$  of **40** and **41**, respectively, are observed, whereas those of compounds **17**, **32**, and **39** are unchanged, indicating that the latter compounds are not transformed by the mEH or other enzymes present in the extract, as are **40** and **41** (*16, 18*). Valpromide was unavailable for direct comparison. Fast-gel filtration (Bio-Spin column P-30, Bio-Rad) of an aqueous solution of mEH (1 nmol of diol formed  $\text{min}^{-1} \text{mL}^{-1}$ ) and elaidamide **32** (100  $\mu\text{M}$ ) resulted in recovery of approximately 90% of the catalytic activity, indicating a rapid dissociation of the inhibitor from the enzyme. To further investigate the mechanism of action of these new inhibitors, we determined the dissociation constants of **17**, **32**, and **39**. A variety of kinetic models were evaluated using Sigma plot. A mixed kinetic model fit the data far better than either competitive or noncompetitive representations. On the Lineweaver–Burk representation for elaidamide **32** (Figure 3), the lines for each inhibitor concentration cross on the left of the  $Y$ -axis, indicating a linear mixed-type inhibition (*28*). This mechanism

**Table 4. Time Effect of Inhibition Potency and Dissociation Constants for Three New Inhibitors and Comparison to Three Previously Described MEH Inhibitors**

Structure	n°	Rat mEH			Human mEH	
		IC <sub>50</sub> (μM) t= 5 min	IC <sub>50</sub> (μM) t= 30 min	K <sub>i</sub> (μM)	α	IC <sub>50</sub> (μM) t= 5 min
	39	6.6 ± 0.3	6.8 ± 0.2	1.0 ± 0.3	3.8 ± 0.4	24 ± 1
	32	1.36 ± 0.01	1.49 ± 0.03	0.07 ± 0.01	7 ± 1	7.7 ± 0.1
	17	2.54 ± 0.04	2.45 ± 0.06	0.24 ± 0.04	5.7 ± 0.1	16.3 ± 0.8
<hr/>						
	40	1.4 ± 0.1	13.9 ± 0.6	Substrate <sup>a</sup>		4.5 ± 0.1
	41	9.7 ± 0.1	18.5 ± 0.7	Substrate <sup>a</sup>		12.4 ± 0.5
	42	4-7 <sup>b</sup>		5.0 <sup>c</sup>		

<sup>a</sup> From ref 2. <sup>b</sup> From ref 29. <sup>c</sup> From ref 19.

of inhibition is described by the equilibrium shown below.



The system is a mixture of partial competitive inhibition and pure noncompetitive inhibition. In this system, the EI complex has an affinity for S that is  $\alpha$ -fold lower than that of E, and similarly, the ES complex has an affinity for I  $\alpha$ -fold lower than that of E. Moreover, the EIS complex is nonproductive (28). The velocity equation for this type of mixed inhibition is given by the following formula.

$$v = \frac{V_m[S]/(1 + [I]/\alpha K_i)}{K_s[(1 + [I]/K_i)/(1 + [I]/\alpha K_i)] + [S]}$$

To calculate  $K_i$  and  $\alpha$ , the slope and the intercept of the Lineweaver–Burk lines obtained for each concentration of inhibitor are plotted as a function of [I] (Figure 3 inset). The intersections of these secondary plots with the X-axis allow the calculation of the two kinetic constants (28). The results that were obtained are displayed in Table 4. For the *N*-dodecylurea 39 and dodecylamine 17, similar kinetic results were obtained, indicating a similar mechanism of action among the three series of compounds. When the similarities in the sEH and mEH catalytic mechanisms are considered, these kinetic data are surprising since urea inhibitors of the sEH give competitive or tight binding competitive kinetics (21). Moreover, X-ray structures of the murine sEH with several inhibitors show the urea pharmacophore interacting with the catalytic aspartic acid (22, 36). This potential mechanism of action for the mEH is consistent with the inactivity of 2-aminonaphthalene 27 as an inhibitor. The good potency of the described MEH inhibitors is confirmed by the fact that the  $K_i$ s obtained are 4–60-fold lower than the  $K_m$

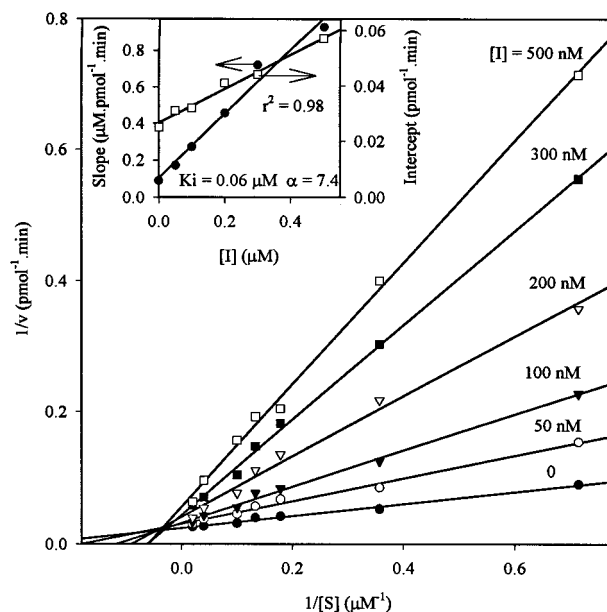


**Figure 3.** Determination of the dissociation constant of elaidamide 32 with RmEH, using [<sup>3</sup>H]-*cis*-stilbene oxide as the substrate. For each inhibitor concentration, the inverse of the velocity is plotted as a function of the inverse substrate concentration. In the inset, the slope (●) and the intercept (□) of the Lineweaver–Burk representations are plotted as a function of the inhibitor concentration, allowing the calculation of  $K_i$  and  $\alpha$ , respectively, as described previously (28). The arrows indicate the axis to which to refer. Similar plots were obtained for compounds 17 and 39. The values shown in Table 4 are the means and standard deviations of three independent measurements of the kinetic constants. In absence of inhibitor, a  $K_m$  of  $4.1 \pm 0.3 \mu\text{M}$  and a  $V_{max}$  of  $39 \pm 1 \text{ pmol min}^{-1}$  per assay were obtained for RmEH hydrolysis of *c*-SO.

obtained for *cis*-stilbene oxide ( $4.1 \pm 0.3 \mu\text{M}$ ). Moreover, the  $K_i$  values obtained for 17, 32, and 39 (Table 4) are 5–70-fold lower than the  $K_i$  of valpromide, the best mEH inhibitor previously described (19). On the basis of the specific activity of the pure enzyme ( $800 \text{ nmol min}^{-1} \text{ mg}^{-1}$ ; 37), the concentration of RmEH ( $0.4 \text{ nmol min}^{-1} \text{ mL}^{-1}$ ) was estimated to be approximately 10 nM in the kinetic assay. The enzyme concentration was confirmed

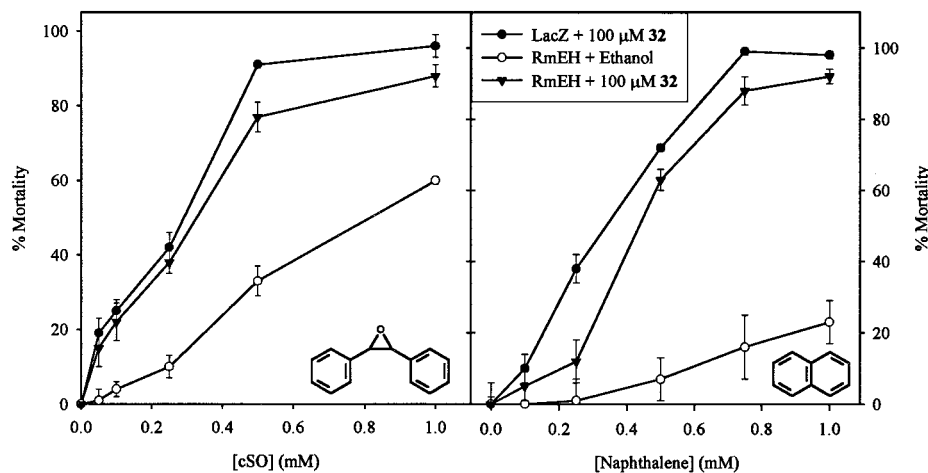


**Figure 4.** Mortality of cultured cells of *S. frugiperda* (Sf-21) expressing the rat mEH in the absence (○) or presence (▼) of 100  $\mu$ M compound **32**. Cells expressing  $\beta$ -galactosidase [Lac Z (●)] were used as a control. (A) Effect of *cis*-stilbene oxide from 0 to 1 mM. RmEH (○) detoxifies *cis*-stilbene oxide (inset) to its diol, and the cytotoxicity of stilbene oxide is enhanced by the mEH inhibitor elaidamide (▼). (B) Effect of naphthalene from 0 to 1 mM on cells coexpressing, in addition to mEH or Lac Z, the P450 1A1/reductase chimeric enzyme. As with *cis*-stilbene oxide, elaidamide enhanced the cytotoxicity of the naphthalene oxide produced in situ by the P450 enzyme. Results are means of three separate experiments; the error bar represents the SD.

by Western blot analysis (not shown) using polyclonal antibodies kindly provided by F. Oesch and M. Arand (University of Mainz, Mainz, Germany) from scanning of the luminograph of the blot; we found that the preparation used for the determination of the kinetic constant contained 3–4 ng of mEH protein in 5  $\mu$ L of solution, which corresponds to a concentration of 0.6–0.8 mg/L, and therefore, using a molecular mass of 50 kDa for mEH, a concentration of 12–15 nM ( $n = 3$ ) was found. For the best inhibitor **32**, the  $K_i$  is only 7-fold greater than the estimated enzyme concentration, indicating a fairly tight association between the enzyme and this inhibitor. The potency of the compounds was tested on the recombinant human mEH (HmEH), under conditions similar to those used for the RmEH (Table 4). The  $IC_{50}$ s for RmEH are overall about 5-fold smaller than for HmEH. However, both enzymes displayed a similar pattern of inhibition, indicating that the rat enzyme is a reasonable model for the development of human mEH inhibitors.

#### Specificity and Cell-Based Effects of Inhibition.

Before the effect of elaidamide **32** on epoxide metabolism was tested, its effects on the activity of carboxylesterases, glutathione transferases, cytosolic EH, microsomal EH, four P450s (1A, 2B, 3A, and 4A1), and a CoA-oxidase from rat liver were evaluated at 100  $\mu$ M (38). Significant inhibition was observed only for microsomal EH activity, suggesting selectivity of this compound for mEH. The effect of elaidamide **32** on the metabolism of two xenobiotics was examined in vitro with cultured cells (Figure 4). For both of the toxicants that were studied, similar results were obtained for the control cells expressing  $\beta$ -galactosidase (Lac Z) in the presence or absence of 100  $\mu$ M **32**, indicating that at this concentration the mEH inhibitor was not toxic. Compared to the Lac Z-expressing cells, the toxicity of *cis*-stilbene oxide (Figure 4A) was strongly reduced by the expression of the RmEH, resulting in increased cell viability ( $LC_{50}$  increased 3-fold). In the presence of 100  $\mu$ M **32**, RmEH protection was lost and toxicity was observed ( $LC_{50}$  similar to that of the Lac Z cells). However, at high toxicant concentrations, the toxicity that was obtained was lower than that observed with Lac Z-expressing cells, suggesting the presence of

residual mEH activity. Because **32** is a noncovalent inhibitor of mEH and it has a partial competitive mechanism of action, partial inhibition occurs especially when  $[S] > [I]$ . For naphthalene (Figure 4B), the expression of the P450 1A1/reductase chimeric enzyme resulted in increased toxicity, which could be overcome by the coexpression of RmEH as observed previously (26). As obtained for *cis*-stilbene oxide, the addition of the inhibitor results in a partial recovery of the toxicity observed for Lac Z-expressing cells.

The new series of mEH inhibitors described herein are able to block mEH activity in vitro. Because valpromide, a previously described less potent mEH inhibitor, was found to influence the in vivo metabolism of carbamazepine epoxide by mEH (19), one could believe that the more potent compounds described herein will also be able to influence the in vivo metabolism of xenobiotics by mEH. Such compounds are good tools for further investigating the physiological and biological role of mEH. Interestingly, sleep-inducing fatty amides were found to inhibit mEH.

**Acknowledgment.** This work was supported in part by NIEHS Grant R01-ES02710, NIEHS Center for Environmental Health Sciences Grant 1P30-ES05707, University of California, Davis, EPA Center for Ecological Health Research Grant CR819658, and by NIH/NIEHS Superfund Basic Research Program P42-ES04699.

**Supporting Information Available:** IR, NMR, and MS data used for structural confirmation. This material is available free of charge via the Internet at <http://pubs.acs.org>.

#### References

- (1) Wixtrom, R. N., and Hammock, B. D. (1985) Membrane-bound and soluble-fraction epoxide hydrolases: methodological aspects. In *Biochemical Pharmacology and Toxicology Vol. 1: Methodological aspects of drug metabolizing enzymes* (Zakim, D., and Vessey, D. A., Eds.) pp 1–93, John Wiley & Sons, New York.
- (2) Oesch, F. (1973) Mammalian epoxide hydrolases: inducible enzymes catalysing the inactivation of carcinogenic and cytotoxic metabolites derived from aromatic and olefinic compounds. *Xenobiotica* **3**, 305–340.
- (3) Siedegård, J., and Ekström, G. (1997) The role of human glutathione transferases and epoxide hydrolases in the metabolism of xenobiotics. *Environ. Health Perspect.* **105**, 791–799.

- (4) Hammock, B. D., Grant, D., and Storms, D. (1997) Epoxide hydrolase. In *Comprehensive Toxicology Vol. 3: Biotransformation* (Guengerich, F. P., Ed.) pp 283–305, Pergamon, Oxford, U.K.
- (5) Zheng, J., Cho, M., Brennan, P., Chichester, C., Buckpitt, A. R., Jones, A. D., and Hammock, B. D. (1997) Evidence for quinone metabolites of naphthalene covalently bound to sulfur nucleophiles of proteins of mouse Clara cell after exposure to naphthalene. *Chem. Res. Toxicol.* **10**, 1008–1014.
- (6) Szeliga, J., and Dipple, A. (1998) DNA adduct formation by polycyclic aromatic hydrocarbon dihydrodiol epoxides. *Chem. Res. Toxicol.* **11**, 1–11.
- (7) Smith, C. A. D., and Harrison, D. J. (1997) Association between polymorphism in gene for microsomal epoxide hydrolase and susceptibility to emphysema. *Lancet* **350**, 630–633.
- (8) Benhamou, S., Reinikainen, M., Bouchary, C., Dayer, P., and Hirvonen, A. (1998) Association between lung cancer and microsomal epoxide hydrolase genotypes. *Cancer Res.* **58**, 5291–5293.
- (9) Miyata, M., Kudo, G., Lee, Y.-H., Yang, T. J., Gelboin, H. V., Fernandez-Salguero, P., Kimura, S., and Gonzalez, F. J. (1999) Targeted disruption of the microsomal epoxide hydrolase gene: microsomal epoxide hydrolase is required for the carcinogenic activity of 7,12-dimethylbenz[ $\alpha$ ]anthracene. *J. Biol. Chem.* **274**, 23963–23968.
- (10) Vogel-Bindel, U., Bentley, P., and Oesch, F. (1982) Endogenous role of microsomal epoxide hydrolase: ontogenesis, induction, inhibition, tissue distribution, immunological behaviour and purification of microsomal epoxide hydrolase with 16 $\alpha$ ,17 $\alpha$ -epoxyandrostene-3-one as substrate. *Eur. J. Biochem.* **126**, 425–431.
- (11) Mésange, F., Sebbar, M., Kedjouar, B., Capdevielle, J., Guillemot, J.-C., Ferrara, P., Bayard, F., Delarue, F., Faye, J.-C., and Poirot, M. (1998) Microsomal epoxide hydrolase of rat liver is a subunit of the anti-oestrogen-binding site. *Biochem. J.* **334**, 107–112.
- (12) Wang, X., Wang, M., Niu, T., Chen, C., and Xu, X. (1998) Microsomal epoxide hydrolase polymorphism and risk of spontaneous abortion. *Epidemiology* **9**, 540–545.
- (13) Stirrat, G. M. (1990) Recurrent miscarriage. I. Definition and epidemiology. *Lancet* **336**, 673–675.
- (14) Alves, C., Von Dippe, P., Amoui, M., and Levy, D. (1993) Bile acid transport into hepatocyte smooth endoplasmic reticulum vesicles is mediated by microsomal epoxide hydrolase, a membrane protein exhibiting two distinct topological orientations. *J. Biol. Chem.* **268**, 20148–20155.
- (15) Von Dippe, P., Amoui, M., Stellwagen, R. H., and Levy, D. (1996) The functional expression of sodium-dependent bile acid transport in Madin-Darby canine kidney cells transfected with the cDNA for microsomal epoxide hydrolase. *J. Biol. Chem.* **271**, 18176–18180.
- (16) Oesch, F., Kaubisch, N., Jerina, D. M., and Daly, J. W. (1971) Hepatic epoxide hydrase. Structure–activity relationships for substrates and inhibitors. *Biochemistry* **10**, 4858–4866.
- (17) Oesch, F., Jerina, D. M., Daly, J. W., and Rice, J. M. (1973) Induction, activation and inhibition of epoxide hydrase: an anomalous prevention of chlorobenzene-induced hepatotoxicity by an inhibitor of epoxide hydrase. *Chem.-Biol. Interact.* **6**, 189–202.
- (18) Magdalou, J., and Hammock, B. D. (1988) 1,2-Epoxycycloalkanes: substrates and inhibitors of microsomal and cytosolic epoxide hydrolases in mouse liver. *Biochem. Pharmacol.* **37**, 2717–2722.
- (19) Kerr, B. M., Rettie, A. E., Eddy, A. C., Loiseau, P., Guyot, M., Wilensky, A. J., and Levy, R. H. (1989) Inhibition of human liver microsomal epoxide hydrolase by valproate and valpromide: *in vitro* correlation. *Clin. Pharmacol. Ther.* **46**, 82–93.
- (20) Draper, A. J., and Hammock, B. D. (1999) Inhibition of soluble and microsomal epoxide hydrolase by zinc and other metals. *Toxicol. Sci.* **52**, 26–32.
- (21) Morisseau, C., Goodrow, M. H., Dowdy, D., Zheng, J., Greene, J. F., Sanborn, J. R., and Hammock, B. D. (1999) Potent urea and carbamate inhibitors of soluble epoxide hydrolases. *Proc. Natl. Acad. Sci. U.S.A.* **96**, 8849–8854.
- (22) Argiriadi, M. A., Morisseau, C., Hammock, B. D., and Christianson, D. W. (1999) Detoxification of environmental mutagens and carcinogens: structure, mechanism, and evolution of liver epoxide hydrolase. *Proc. Natl. Acad. Sci. U.S.A.* **96**, 10637–10642.
- (23) Armstrong, R. N. (1999) Kinetic and chemical mechanism of epoxide hydrolase. *Drug Metab. Rev.* **31**, 71–86.
- (24) Roe, E. T., Scanlan, J. T., and Swern, D. (1949) Fatty acid amides. I. Preparation of amides of oleic and the 9,10-dihydroxystearic acids. *J. Am. Chem. Soc.* **71**, 2215–2220.
- (25) Debernard, S., Morisseau, C., Severson, T. F., Feng, L., Wojtasek, H., Prestwich, G. D., and Hammock, B. D. (1998) Expression and characterization of the recombinant juvenile hormone epoxide hydrolase (JHEH) from *Manduca sexta*. *Insect Biochem. Mol. Biol.* **28**, 409–419.
- (26) Grant, D. F., Greene, J. F., Pinot, F., Borhan, B., Moghaddam, M. F., Hammock, B. D., McCutchen, B., Ohkawa, H., Luo, G., and Guenther, T. M. (1996) Development of an *in situ* toxicity assay system using recombinant baculoviruses. *Biochem. Pharmacol.* **51**, 503–515.
- (27) Yamada, T., Morisseau, C., Maxwell, J. E., Argiriadi, M. A., Christianson, D. W., and Hammock, B. D. (2000) Biochemical evidence of the involvement of tyrosine in epoxide activation during the catalytic cycle of epoxide hydrolase. *J. Biol. Chem.* **275**, 23082–23088.
- (28) Segel, I. H. (1993) *Enzyme kinetics: behavior and analysis of rapid equilibrium and steady-state enzyme systems*, pp 170–176, John Wiley & Sons, New York.
- (29) Kerr, B. M., and Levy, R. H. (1989) Unsubstituted amides: new class of potent inhibitors of human microsomal epoxide hydrolase. *Drug Metab. Dispos.* **18**, 540–542.
- (30) Spiegelstein, O., Kroetz, D. L., Levy, R. H., Yagen, B., Hurst, S. I., Levi, M., Haj-Yehia, A., and Bialer, M. (2000) Structure–activity relationship of human microsomal epoxide hydrolase inhibited by amide and acid analogues of valproic acid. *Pharm. Res.* **17**, 216–221.
- (31) Cravatt, B. F., Prospero-Garcia, O., Siuzdak, G., Gilula, N. B., Henriksen, S. J., Boger, D. L., and Lerner, R. A. (1995) Chemical characterization of a family of brain lipids that induce sleep. *Science* **268**, 1506–1509.
- (32) Calignano, A., La Rana, G., Giuffrida, A., and Piomelli, D. (1998) Control of pain initiation by endogenous cannabinoids. *Nature* **394**, 277–281.
- (33) Teisier, E., Fennrich, S., Strazielle, N., Daval, J.-L., Ray, D., Schlosshauer, B., and Ghersi-Egea, J.-F. (1998) Drug metabolism *in vitro* organotypic and cellular models of mammalian central nervous system: activities of membrane-bound epoxide hydrolase and NADPH-cytochrome P-450 (c) reductase. *Neurotoxicology* **19**, 347–356.
- (34) Boger, D. L., Patterson, J. E., and Jin, Q. (1998) Structural requirements for 5-HT<sub>2A</sub> and 5-HT<sub>1A</sub> serotonin receptor potentiation by the biologically active lipid oleamide. *Proc. Natl. Acad. Sci. U.S.A.* **95**, 4102–4107.
- (35) Boger, D. L., Patterson, J. E., Guan, X., Cravatt, B. F., Lerner, R. A., and Gilula, N. B. (1998) Chemical requirements for inhibition of gap junction communication by the biologically active lipid oleamide. *Proc. Natl. Acad. Sci. U.S.A.* **95**, 4810–4815.
- (36) Argiriadi, M. A., Morisseau, C., Goodrow, M. H., Dowdy, D. L., Hammock, B. D., and Christianson, D. W. (2000) Binding of alkylurea inhibitors to epoxide hydrolase implicates active site tyrosines in substrate activation. *J. Biol. Chem.* **275**, 15265–15270.
- (37) Bentley, P., Oesch, F., and Tsugita, A. (1975) Properties and amino acid composition of pure epoxide hydratase. *FEBS Lett.* **59**, 296–299.
- (38) Morisseau, C., Derbel, M., Lane, T. R., Stoutamire, D., and Hammock, B. D. (1999) Differential induction of hepatic drug-metabolizing enzymes by fenvaleric acid in male rats. *Toxicol. Sci.* **52**, 148–153.

TX0001732